

# Formation of two particular structures between $\beta$ -cyclodextrin and bifonazole: $\beta$ -cyclodextrin–bifonazole and $(\beta\text{-cyclodextrin})_i\text{-bifonazole}$ (where $2 < i < 3$ )



Nadia Morin,<sup>\*a</sup> Grégorio Crini,<sup>b</sup> Cesare Cosentino,<sup>c</sup> Joëlle Millet,<sup>d</sup> Joël Vebrel<sup>b</sup> and Jean-Charles Rouland<sup>a</sup>

<sup>a</sup> Laboratoire de Chimie Physique et Minérale, Faculté de Médecine et de Pharmacie, Place Saint Jacques, 25030 Besançon Cedex, France

<sup>b</sup> Centre de Spectrométrie, Université de Franche-Comté, 16, Route de Gray, 25000 Besançon, France

<sup>c</sup> Istituto di Chimica e Biochimica "G. Ronzoni" 81, Via G. Colombo, 20133 Milano, Italy

<sup>d</sup> Laboratoire de Pharmacie Galénique, Faculté de Médecine et de Pharmacie, Place Saint Jacques, 25030 Besançon Cedex, France

Received (in Cambridge, UK) 16th February 1999, Accepted 31st August 1999

This paper deals with inclusion compound formation between  $\beta$ -cyclodextrin ( $\beta$ -CD) and bifonazole, an antimycotic hydrophobic imidazole derivative. High performance liquid chromatography (HPLC) was used in order to measure the solubility of this drug as a function of the quantity of cyclodextrin in the samples. According to the classification of Higuchi and Connors, an A type solubility diagram was obtained, revealing the formation of soluble inclusion compound(s). Differential scanning calorimetry (DSC) was used for the first time, in order to draw binary phase and Tammann diagrams between  $\beta$ -cyclodextrin and bifonazole. The experimental results demonstrated the formation of two binary compounds,  $\beta$ -cyclodextrin–bifonazole and  $(\beta\text{-cyclodextrin})_i\text{-bifonazole}$  (where  $2 < i < 3$ ). The two compounds have been characterised using solid state nuclear magnetic resonance (NMR) spectroscopy. Different NMR spectra have been obtained, which indicate that the first compound is an inclusion compound and the second may be a crystallised compound, in which the bifonazole is not necessarily included in the cyclodextrin internal cavity.

## 1. Introduction

Cyclodextrins (CDs), which are torus-shaped cyclic oligosaccharides consisting of six or more  $\alpha$ -(1,4)-linked D-glucopyranose units are one of the well known host molecules capable of forming an inclusion complex (host–guest complex) with a wide variety of organic molecules or so-called guest molecules.<sup>1</sup> CDs receive considerable attention as they are able to modify the physical and chemical properties of the included drugs, such as an increasing aqueous solubility to lipophilic compounds.<sup>1</sup> Jarho *et al.*<sup>2</sup> investigated the increase of anandamine aqueous solubility and stability by complexation with hydroxypropyl- $\beta$ -cyclodextrin (HP- $\beta$ -CD). Chun and Yun<sup>3</sup> studied the inclusion complexation of hydrocortisone butyrate with CDs in aqueous solution and in the solid state. The solubility increase of hydrocortisone butyrate in the presence of CDs in water was in the order dimethyl- $\beta$ -cyclodextrin (DM- $\beta$ -CD)  $\gg$   $\gamma$ -cyclodextrin ( $\gamma$ -CD)  $>$   $\beta$ -CD  $>$   $\alpha$ -cyclodextrin ( $\alpha$ -CD). The dissolution rate of the DM- $\beta$ -CD solid complex was extremely rapid compared with those of  $\alpha$ -,  $\beta$ - and  $\gamma$ -CD solid complexes. Esclusa-Diaz *et al.*<sup>4</sup> have plotted the phase solubility diagrams of glibenclamide in the presence of 2-HP- $\beta$ -CD in aqueous medium. According to the phase solubility results, drug solubility in an alkaline medium was greatly improved by inclusion with HP- $\beta$ -CD, whereas in an acid medium inclusion with HP- $\beta$ -CD had no appreciable effect. Guyot *et al.*<sup>5</sup> observed that the solubility and dissolution rate of norfloxacin were significantly increased with poly(ethylene glycol) (PEG) solid dispersions and cyclodextrin complexes. However, enhancement was not statistically different either among various cyclodextrin complexes, or between solid dispersions and cyclodextrin complexes.

Imidazole and triazole derivatives were used pharmacologic-

ally for the treatment of onychomycosis. Nevertheless, these hydrophobic compounds had a weak penetration into hydrophilic human nail matrices. Their inclusion in the apolar cyclodextrin cavity could improve this penetration, considering the hydrophilic character of the exterior of the cyclodextrin which is made up of a great number of hydroxy groups. Pedersen *et al.*<sup>6</sup> have measured by high performance liquid chromatography (HPLC) the solubility of two imidazole derivatives, miconazole and econazole in the presence of cyclodextrins. The solubility curves between a series of imidazoles and  $\beta$ -CD have been measured by Van Doorne *et al.*<sup>7,8</sup> determining the quantities of dissolved drugs spectrophotometrically.

In this paper, the inclusion compound formation between  $\beta$ -cyclodextrin and bifonazole was investigated by plotting solubility curves, binary phase diagrams and NMR spectra. The solubility diagram corresponds to the plot of the total mole concentration of bifonazole dissolved (determined by HPLC) against the mole concentration of  $\beta$ -CD in samples.<sup>9</sup> Binary phase and Tammann diagrams correspond respectively to the plot of temperatures and enthalpy variations ( $\Delta H$ ) versus the bifonazole mole fraction in the samples.

## 2. Experimental

### 2.1. Apparatus

The HPLC system consisted of a Waters HPLC pump 501 (Saint-Quentin, Yvelines, France), an Interchim rheodyne injection valve, model 7125 (Montluçon, France), fitted with a 20  $\mu$ L sample loop and a Shimadzu SPD-10A (Touzart-Matignon, Vitry sur Seine, France) variable wavelength UV spectrophotometer detector (Nogent sur Marne, France). A Lichrocart<sup>®</sup> 125 mm  $\times$  4 mm id column (5  $\mu$ m particle size)

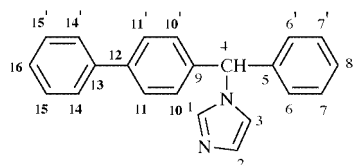


Fig. 1 Bifonazole structure.

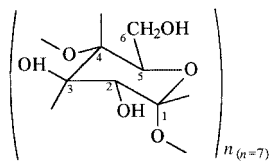


Fig. 2  $\beta$ -Cyclodextrin structure.

(Merck, Darmstadt, Germany) was used. The mobile phase rate was fixed at  $1 \text{ mL min}^{-1}$  and the wavelength at 230 nm.

Differential scanning calorimetry (DSC) measurements were carried out using a heat flux T.A. 2000 Instruments DuPont (Paris, France) apparatus which was calibrated for temperature and enthalpy by melting high purity indium. The instrument was flushed with nitrogen which is known by its density and low thermal conductivity. Samples of 5 to 10 mg were transferred into aluminium crucibles which were sealed and weighed. The cover had three orifices to allow vaporisation. Experiments were performed with a heating rate of  $10 \text{ deg min}^{-1}$  over the temperature range  $20\text{--}300 \text{ }^\circ\text{C}$ .

Complementarily, X-ray diffraction patterns were performed with a CGR X-ray powder diffractometer using the wavelength of Cu-K $\alpha$  radiation ( $\lambda = 1.5406 \text{ \AA}$ ).

Cross polarisation and magic angle spinning solid state nuclear magnetic resonance (CPMAS NMR) measurements were used for the characterisation of the samples. The CPMAS spectra were recorded with a Bruker AC-300 spectrometer operating at 75.47 MHz and 303 K. The CPMAS utilisation conditions have been described in a previous work.<sup>10</sup> Before experimentation, the  $\beta$ -CD sample was recrystallised from water and kept overnight under vacuum at  $110 \text{ }^\circ\text{C}$ . Bifonazole and complex samples, prepared by coprecipitation (see Section 3.2), were also kept under vacuum at  $60 \text{ }^\circ\text{C}$  for 20 h. The ROESY spectrum was obtained on a Bruker AMX 600 spectrometer by courtesy of Dr Perly (CEA, Gif sur Yvette).

## 2.2. Solvents and samples

HPLC grade methanol (Carlo Erba, Val de Reuil, France) and acetone (Prolabo, Paris, France) were used without further purification. Water was obtained from an Elgastat option I water purification system (Odil, Talant, France), fitted with a reverse osmosis cartridge. The mobile phase used for the study was a methanol–aqueous phosphate buffer (75/25% v/v) mixture. The phosphate buffer, for which the pH value was equal to 7, was composed of 0.01 M diammonium hydrogen phosphate, 0.02 M ammonium dihydrogen phosphate and 0.0005 M *n*-nonylamine to avoid peak tailing. Bifonazole (Fig. 1), which was obtained from Sigma (Saint Quentin Fallavier, France), was dissolved in pure acetone for HPLC analysis. Retention times were measured using a Merck D2500 chromatointegrator.  $\beta$ -CD (Fig. 2) was provided by the Roquette Laboratories (Lestrem, France).

## 3. Methods

### 3.1. Solubility study

The experimental procedure is shown schematically in Fig. 3. To 10 mL of water containing various  $\beta$ -cyclodextrin quantities, from 0 to 16 mM, 10 mg of the antimycotic drug was added. The suspensions were shaken with a magnetic stirrer, for

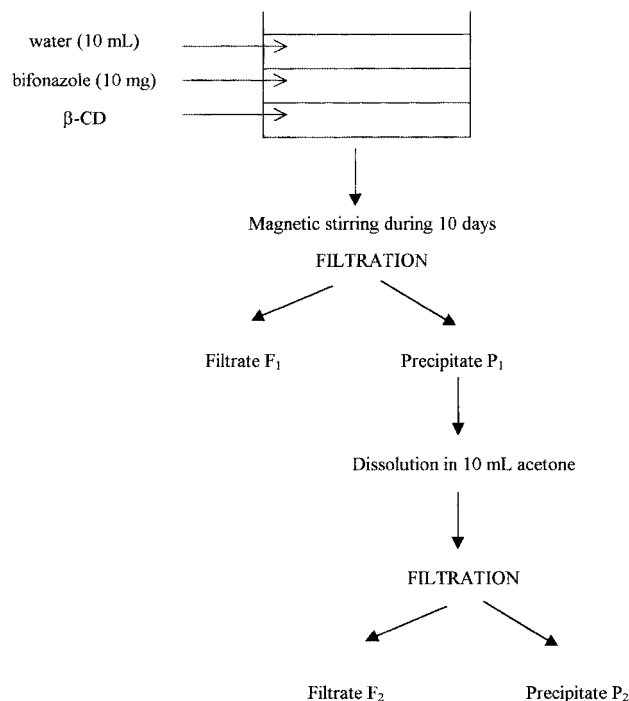


Fig. 3 Schematic experimental procedure.

ten days (until the equilibrium was reached<sup>6</sup>), at  $27 \text{ }^\circ\text{C}$ . Then they were filtered through a  $0.2 \text{ }\mu\text{m}$  Sartorius cellulose acetate membrane filter (Göttingen, Germany). The filtrates,  $F_1$ , were isolated. The removed precipitates,  $P_1$ , were dissolved in 10 mL acetone, giving sometimes new precipitates,  $P_2$ , which were filtered in order to isolate the  $F_2$  filtrates. Finally,  $F_2$  were assessed by HPLC as described in the Experimental section. They corresponded to the quantity of non dissolved drug in water. By subtracting from the known initial introduced drug quantity, the amount which was dissolved was determined. Consequently, a Higuchi and Connors diagram has been constructed by plotting, on the vertical axis, the total mole concentration of substrate *S* (bifonazole) dissolved against the mole concentration of ligand *L* ( $\beta$ -CD).<sup>9</sup> Solubility curves are observed to fall into two main classes, type A and type B, with some variations within the classes.

Type A diagrams, for which the solubility of the substrate increased with increasing quantities of ligand, indicated the formation of soluble complexes between *S* and *L*. An  $A_L$  diagram was represented by a linear increase, while  $A_N$  and  $A_P$  diagrams were represented by negative and positive curvatures in the line respectively.

Type B diagrams were observed when insoluble complexes were formed. The  $B_S$  diagram was identical, in the first part of curve, to type A diagrams, already discussed: the solubility of *S* was increased, due to the soluble complex formation between *S* and *L*. Then, the solubility limit was reached; this complex precipitated and the solution was supersaturated. The  $B_I$  diagram was interpreted in the same manner, with the difference that the complex formed was so insoluble that the initial rise of solubility shown in the  $B_S$  diagram was not detectable.

We note that  $\beta$ -CD was different from other complexing agents studied by Higuchi and Connors, such as caffeine and nicotinamide, because of its internal cavity.

### 3.2. Binary phase diagram

Solid complexes were prepared by the coprecipitation method.<sup>11</sup> Solutions of  $\beta$ -CD (4% w/w) prepared with distilled water were heated to  $65 \text{ }^\circ\text{C}$ . 10 mg of bifonazole were dissolved in 25 mL acetone and added to the  $\beta$ -CD aqueous solutions. The final solutions were then mixed continuously with a magnetic stirrer

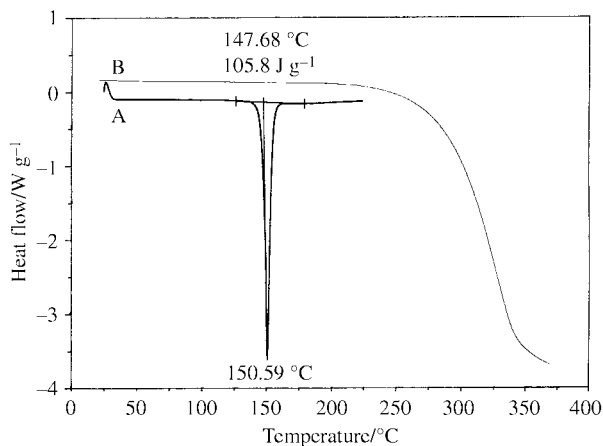


Fig. 4 Bifonazole thermogram (A) and thermogravimetric analysis (B) curves.

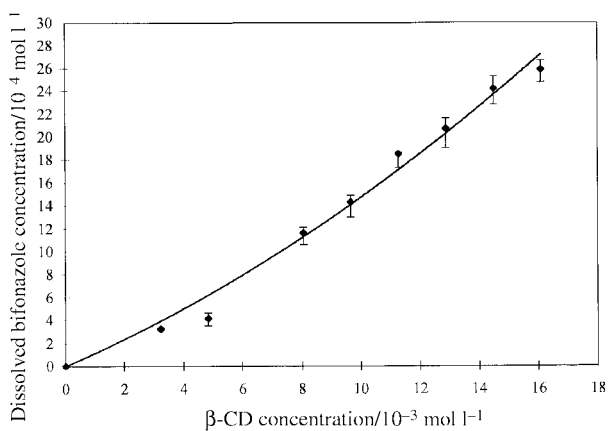


Fig. 5 Solubility diagram of bifonazole.

and heated to 65 °C. The organic solvent was allowed to evaporate and the mixtures were cooled to 5 °C. The crystals were separated by filtration through 0.2 μm Sartorius cellulose acetate membrane filters. Then, the samples were dried and stored at room temperature. The whole range of compositions was prepared and analysed by DSC by steps of bifonazole mole fractions  $x = 0.05$  between 0 and 1. In order to permit the accurate evaluation of endothermic effects and to allow the escape of water and volatile compounds during the heating process, a thermal cycle was set up.<sup>12,13</sup> The samples were first heated to 135 °C and kept at this temperature for 5 min, then allowed to cool to 100 °C and finally rescanned up to 300 °C. Thus, the endothermic invariance peaks observed in the β-CD–bifonazole binary systems were isolated from the large endothermic peak corresponding to the loss of water molecules which represented a component of the β-CD molecules.

## 4. Results and discussion

### 4.1. Solubility study

The thermograms and X-ray diffractograms of P<sub>2</sub> precipitates revealed that P<sub>2</sub> precipitates corresponded to β-CD. The released quantities were variable and were a function of the excess initially introduced. As predicted previously, the thermal analysis carried out on the F<sub>2</sub> solid residues, obtained after acetone evaporation, revealed that it was bifonazole (in excess in the initial samples) because of the presence of an endothermic peak at 147.7 °C corresponding to the bifonazole melting (Fig. 4).

Fig. 5 shows the solubility curve of bifonazole with β-CD. The solubility of bifonazole was apparently increased by the

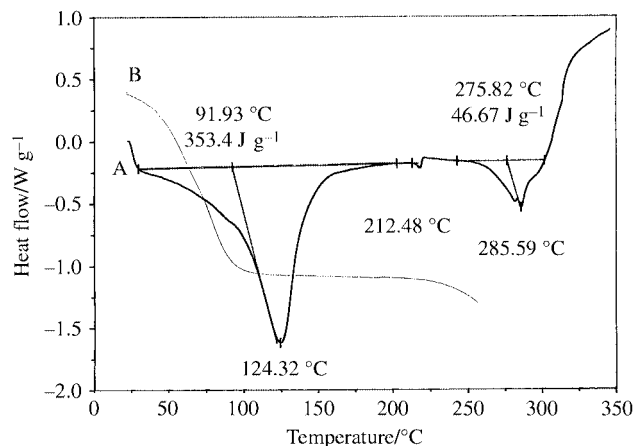


Fig. 6 β-CD thermogram (A) and thermogravimetric analysis (B) curves.

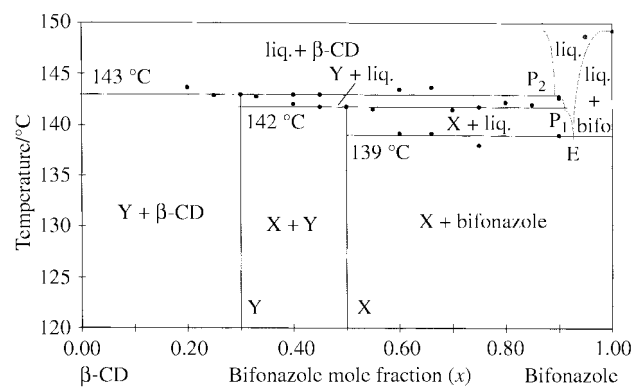
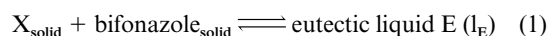


Fig. 7 Binary phase diagram between β-CD and bifonazole.

presence of β-CD corresponding to an A type diagram and indicating the formation of soluble complex(es) between β-CD and bifonazole.

### 4.2. Binary phase diagrams

Fig. 6 shows the DSC and thermogravimetric analysis thermograms of β-CD. Three endothermic peaks are observed. The first peak, between 20 and 150 °C corresponds to the dehydration of β-CD. The experimental water content indicates that β-CD contains 12 moles of crystallisation water which are lost at 150 °C. This result is in good accordance with those reported by Steiner *et al.*<sup>14</sup> and Bilal *et al.*<sup>15</sup> The second small endothermic peak at 213 °C, without any weight loss, represents a process corresponding probably to a molecular reorganisation of β-CD as described by Yilmaz *et al.*<sup>16</sup> The third stage is related to the decomposition of the β-CD structure. Decomposition starts at 288 °C and the rapid weight loss continues up to 325 °C. Fig. 4 shows the DSC and thermogravimetric analysis thermograms of bifonazole. An endothermic peak appears at 147.7 °C, corresponding to the melting of the pure product. Bifonazole is a stable compound: its decomposition starts only above 225 °C. Fig. 7 represents the binary phase diagrams between β-CD and bifonazole. The β-CD–bifonazole samples prepared by coprecipitation were submitted to the thermal cycle described in the Methods section.<sup>11</sup> 21 samples were analysed, with bifonazole mole fractions from 0 to 1, by steps of 0.05. Three invariants are observed. The first one, at 139 °C is attributed to the eutectic equilibrium (1), where X is a definite



compound with a bifonazole mole fraction,  $x$ , equal to 0.50. Also, its stoichiometry is β-CD–bifonazole. The second invariant, observed at 142 °C, is attributed to the peritectic

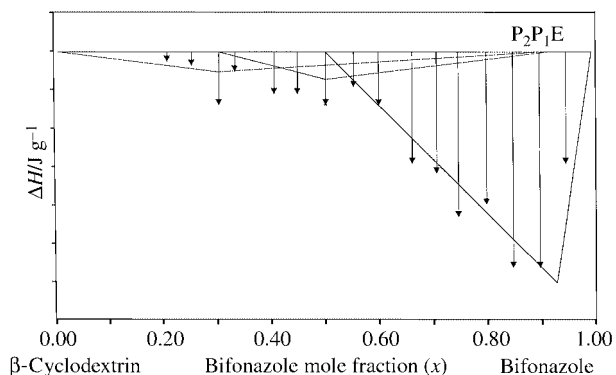


Fig. 8 Tammann diagram between  $\beta$ -cyclodextrin and bifonazole.

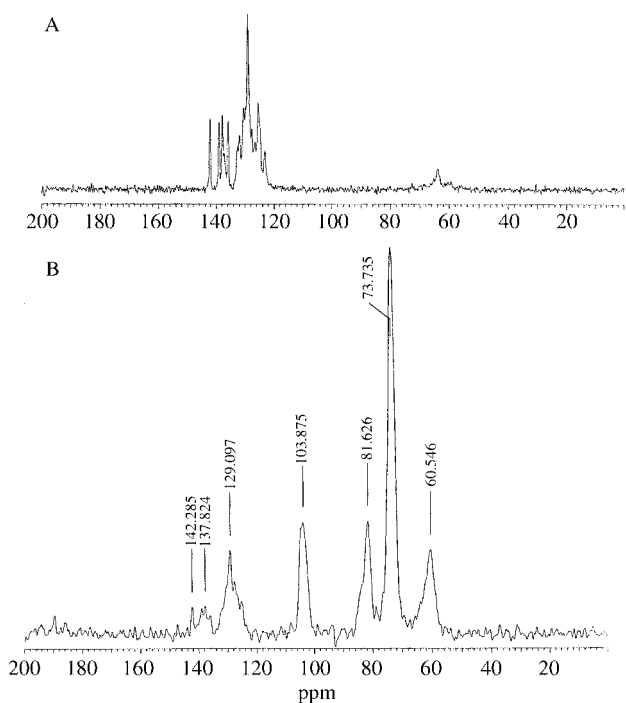
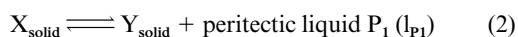


Fig. 9 CPMAS  $^{13}\text{C}$  NMR spectra of bifonazole (A) and  $\beta$ -CD-bifonazole (B).

equilibrium (2), where Y is a definite compound with a



bifonazole mole fraction,  $x$ , equal to 0.30. Also, its stoichiometry is  $(\beta\text{-CD})_i\text{-bifonazole}$  (where  $2 < i < 3$ ). The last invariant, observed at 143 °C, is attributed to the second peritectic equilibrium (3).



As the three temperatures given above were close, measurement of the enthalpies of the three invariant equilibria was not possible. Thus, a Tammann diagram was plotted in which, for each composition, the whole thermal effect was taken into account (Fig. 8). However, the different slopes which are shown in this diagram suggest that each  $\Delta H$  value results in the superposition of two or three thermal effects. In Fig. 8, three Tammann diagrams are reconstituted for the three invariant equilibria. The compositions of the eutectic and peritectic liquids can be determined using these Tammann diagrams:  $x_{\text{I}_e} \approx 0.93$ ,  $0.90 \leq x_{\text{P}_1}$ ,  $x_{\text{P}_2} < 0.93$ .

#### 4.3. NMR study

The CPMAS  $^{13}\text{C}$  NMR spectrum of the  $\beta$ -CD-bifonazole (X)

Table 1 Chemical shift data (in ppm) of free  $\beta$ -CD, free bifonazole and  $\beta$ -CD and bifonazole in the compound

attribution	$\beta$ -CD		attribution	bifonazole	
	free	in the X compound		free	in the X compound
C <sup>1</sup>	103.9	103.9	C <sup>9</sup>	142.3	142.3
	102.9		C <sup>5</sup>	139.1	138.5
	102.1		C <sup>13</sup>	138.0	137.8
	101.6		C <sup>12</sup>	136.5	136.5
	100.4		C <sup>1</sup>	136.0	
	99.6		C <sup>15</sup>	132.9	
	84.3		C <sup>2,7</sup>	132.0	
C <sup>4</sup>	82.8	81.6	C <sup>6</sup>	130.6	
	81.3		C <sup>8</sup>	130.0	
	78.0		C <sup>10</sup>	129.2	129.1
	74.7		C <sup>16</sup>	127.8	
	76.9		C <sup>11</sup>	126.7	127.0
	76.0		C <sup>14</sup>	125.5	125.4
	74.8		C <sup>3</sup>	123.2	
C <sup>3</sup>	63.9	60.6	C <sup>4</sup>	64.0	
	62.5				
	61.4				
	60.1				

compound is shown in Fig. 9. For comparison, the spectrum of free bifonazole (non complexed) is also given in this Figure. The chemical shift data obtained for  $\beta$ -CD are listed in Table 1 and are in agreement with literature data.<sup>10,17-21</sup> The  $\beta$ -CD sample shows a high degree of crystallinity (which may also include different forms) as revealed by the number of resonances due to C-1, C-4 and C-6 atoms of the glucose unit in the  $^{13}\text{C}$  solid state spectra.<sup>10</sup> By analogy with the chemical shifts in solution, the different carbon resonances of bifonazole were assigned and reported in Table 1.<sup>22</sup> The CPMAS spectrum of the  $\beta$ -CD-bifonazole compound (X) (Fig. 9B) shows the peaks of a disordered  $\beta$ -CD (broad signals) in the range 50–110 ppm and those, rather well defined, of bifonazole. The chemical shift data obtained for  $\beta$ -CD and bifonazole in the X compound are presented in Table 1. The  $\beta$ -CD carbon resonances are less well-resolved than in free  $\beta$ -CD,<sup>10</sup> but the main changes are observed at the level of bifonazole signals in the range 115–145 ppm. Bifonazole gives rise to seven resolved carbon signals at 142.3, 138.5, 137.8, 136.5, 129.1, 127.0 and 125.4 ppm, instead of fifteen (Table 1 and Fig. 9A). These effects can be attributed to the formation of an inclusion compound. In addition, the CPMAS spectrum of a mixture of  $\beta$ -CD and bifonazole in the same proportions as in the complex ( $x = 0.50$ ) corresponds to the simple superposition of free  $\beta$ -CD and bifonazole spectra. In the same manner, the CPMAS spectrum of the  $(\beta\text{-CD})_i\text{-bifonazole}$  (where  $2 < i < 3$ ) compound (Y) corresponds to the superposition of free  $\beta$ -CD and bifonazole spectra, indicating that  $(\beta\text{-CD})_i\text{-bifonazole}$  (where  $2 < i < 3$ ) is a binary compound, in which bifonazole is not included in the  $\beta$ -CD cavity. In addition, a ROESY spectrum in  $\text{D}_2\text{O}$  for the X compound shows an evident correlation between the internal protons of the  $\beta$ -CD and the protons of bifonazole<sup>22</sup> in the 3.6–4 ppm region as shown in Fig. 10. Using these first NMR results, it is reasonable to ascribe these effects to the formation of an inclusion complex between  $\beta$ -CD and bifonazole in the X compound. This hypothesis is also confirmed by the fact that in the ROESY spectrum for the Y compound, there are no correlations. Relaxation experiments and an NMR study using variable temperatures are in progress to confirm this hypothesis.<sup>22</sup> Similar results have been reported for other guest molecules complexed with  $\beta$ -CD.<sup>18,21</sup>

#### 5. Conclusions

In this paper, the inclusion compound formation between

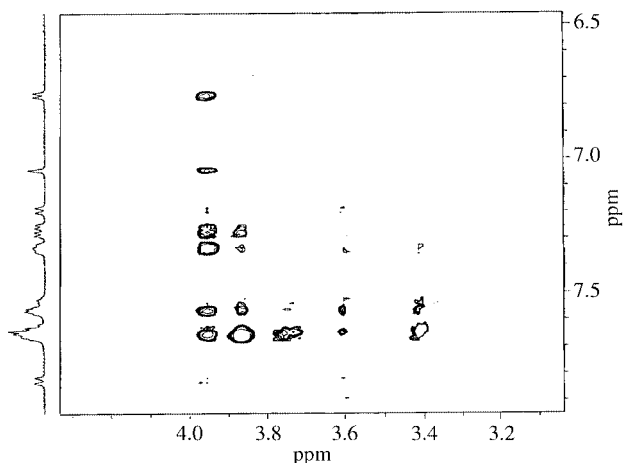


Fig. 10 ROESY spectrum in D<sub>2</sub>O for X compound.

$\beta$ -cyclodextrin and bifonazole was studied. The method of Higuchi and Connors was used first, and revealed the formation of soluble structures between  $\beta$ -CD and bifonazole, without giving more information about the nature of these structures. The purpose of this work was to prove, employing thermal analysis, the existence of two new compounds which were formed between  $\beta$ -CD and bifonazole:  $\beta$ -cyclodextrin–bifonazole and ( $\beta$ -cyclodextrin)<sub>i</sub>–bifonazole (where  $2 < i < 3$ ). The first NMR results indicate that the first compound is an inclusion compound, in which the bifonazole is totally or only partially included in the cyclodextrin cavity and the second one a simple binary compound without bifonazole inclusion in the cyclodextrin internal cavity. Their phase domains and their simultaneous solubilities have been determined: generally,  $\beta$ -CD increased bifonazole solubility. These two compounds may be important in onychomycosis therapy, as they are more soluble in water than bifonazole alone. Thus, they could penetrate more easily the superficial hydrophilic nail keratins. Thus, cyclodextrin could increase the penetration and/or adsorption of imidazole derivatives (such as bifonazole) through human nail matrices.

## References

- 1 J. Szejtli, *Cyclodextrins and their inclusion complexes*, Akadémiai Kiadó, Budapest, 1982.
- 2 P. Jarho, A. Urtti, K. Järvinen, D. W. Pate and T. Järvinen, *Life Sci.*, 1996, **58**, 181.
- 3 I. K. Chun and D. S. Yun, *Int. J. Pharm.*, 1993, **96**, 91.
- 4 M. T. Esclusa-Diaz, J. J. Torres-Labandeira, M. Kata and J. L. Vila-Jato, *Eur. J. Pharm. Sci.*, 1994, **1**, 291.
- 5 M. Guyot, F. Fawaz, J. Bildet, F. Bonini and A. M. Laguény, *Int. J. Pharm.*, 1995, **123**, 53.
- 6 M. Pedersen, M. Edelsten, V. F. Nielsen, A. Scarpellini, S. Skytte and C. Slot, *Int. J. Pharm.*, 1993, **90**, 247.
- 7 H. Van Doorne, E. H. Bosch and C. F. Lerk, in *Proceedings of the fourth international symposium on cyclodextrins*, O. Huber and J. Szejtli (Eds.), Kluwer Academic Publishers, 1988, pp. 285–291.
- 8 H. Van Doorne, E. H. Bosch and C. F. Lerk, *Pharm. Weekbl. Sci. Ed.*, 1988, **10**, 80.
- 9 T. Higuchi and K. A. Connors, *Adv. Anal. Chem. Instrum.*, 1965, **4**, 117.
- 10 G. Crini, C. Cosentino, S. Bertini, A. Naggi, G. Torri, C. Vecchi, L. Janus and M. Morcellet, *Carbohydr. Res.*, 1998, **308**, 37.
- 11 V. T. Yilmaz, A. Karadag and H. İçbudak, *Thermochim. Acta*, 1995, **261**, 107.
- 12 F. Giordano, M. Pavan, J. X. Yan, A. La Manna and G. P. Bettinetti, *On the inclusion evidence of drugs with cyclodextrins by microcalorimetry*, 5th International Conference on Pharmaceutical Technology, Paris, May, 1989.
- 13 E. Redenti, T. Peveri, M. Zanol, P. Ventura, G. Gnappi and A. Montenero, *Int. J. Pharm.*, 1996, **129**, 289.
- 14 T. Steiner, A. M. Moreira da Silva, J. J. C. Teixeira-Dias, J. Müller and W. Saenger, *Angew. Chem., Int. Ed. Engl.*, 1995, **34**, 1452.
- 15 M. Bilal, C. De Brauer, P. Claudy, P. Germain and J. M. Létoffé, *Thermochim. Acta*, 1995, **249**, 63.
- 16 V. T. Yilmaz, A. Karadag and H. İçbudak, *Thermochim. Acta*, 1995, **261**, 107.
- 17 Y. Inoue, T. Okuda and R. Chujo, *Carbohydr. Res.*, 1985, **141**, 179.
- 18 Y. Inoue, F. Kuan and R. Chujo, *Carbohydr. Res.*, 1987, **159**, 1.
- 19 I. Furo, I. Pocsik, K. Tompa, R. Teeaar and E. Lippmaa, *Carbohydr. Res.*, 1987, **166**, 27.
- 20 S. J. Heyes, N. J. Clayden and C. M. Dobson, *Carbohydr. Res.*, 1992, **233**, 1.
- 21 H. Sfihi, A. P. Legrand, J. Doussot and A. Guy, *Colloids Surf. A*, 1996, **115**, 115.
- 22 N. Morin, G. Crini, B. Perly and J.-C. Rouland, unpublished work.

Paper 9/01254K